

Article

## Tensile and Compressive Responses of Ceramic and Metallic Nanoparticle Reinforced Mg Composites

Khin Sandar Tun <sup>1,†</sup>, Wai Leong Eugene Wong <sup>2</sup>, Quy Bau Nguyen <sup>1</sup> and Manoj Gupta <sup>1,\*</sup>

<sup>1</sup> Department of Mechanical Engineering, National University of Singapore, 9 Engineering Drive 1, 117576, Singapore; E-Mails: sandar\_k\_tun@ite.edu.sg (K.S.T.); mpenqb@nus.edu.sg (Q.B.N.)

<sup>2</sup> School of Mechanical and Systems Engineering, Newcastle University International Singapore (NUIS), 180 Ang Mo Kio Ave 8, 569830, Singapore; E-Mail: eugene.wong@ncl.ac.uk

<sup>†</sup> Current address: Technology Development Centre, ITE College Central, 2 Ang Mo Kio Drive, 567720, Singapore.

\* Author to whom correspondence should be addressed; E-Mail: mpegm@nus.edu.sg; Tel.: +65-6516-6358; Fax: +65-6779-1459.

Received: 2 April 2013; in revised form: 24 April 2013 / Accepted: 27 April 2013 /

Published: 7 May 2013

---

**Abstract:** In the present study, room temperature mechanical properties of pure magnesium, Mg/ZrO<sub>2</sub> and Mg/(ZrO<sub>2</sub> + Cu) composites with various compositions are investigated. Results revealed that the use of hybrid (ZrO<sub>2</sub> + Cu) reinforcements in Mg led to enhanced mechanical properties when compared to that of single reinforcement (ZrO<sub>2</sub>). Marginal reduction in mechanical properties of Mg/ZrO<sub>2</sub> composites were observed mainly due to clustering of ZrO<sub>2</sub> particles in Mg matrix and lack of matrix grain refinement. Addition of hybrid reinforcements led to grain size reduction and uniform distribution of hybrid reinforcements, globally and locally, in the hybrid composites. Macro- and micro- hardness, tensile strengths and compressive strengths were all significantly increased in the hybrid composites. With respect to unreinforced magnesium, failure strain was almost unchanged under tensile loading while it was reduced under compressive loading for both Mg/ZrO<sub>2</sub> and Mg/(ZrO<sub>2</sub> + Cu) composites.

**Keywords:** metal matrix composites; microwave sintering; mechanical properties; microstructure; scanning electron microscopy; X-ray diffraction

---

## 1. Introduction

Magnesium is the lightest metallic construction material which is ~35% lighter than aluminum. Owing to its low density, magnesium offers high specific mechanical properties. In addition, magnesium has other favorable advantages including high damping capacity, high dimensional stability, good machinability, good electromagnetic shielding characteristics and recyclability. With these beneficial properties, magnesium becomes an attractive material for manufacturing lighter components/products for diverse applications. In practical and commercial applications, magnesium is mostly used in the form of alloys [1,2]. With the advent of composite technology, researchers have also made extensive studies on the development of high performance magnesium composites. Magnesium composites that were synthesized mostly contained micron-sized particles comprising of ceramic reinforcements such as carbides, oxides, nitrides and borides and metallic reinforcement such as Ti, Cu and Ni [3–6]. While the strengths in magnesium composites can be improved using micron particles, the ductility was inevitably decreased. Previous studies [7–11] on magnesium nanocomposites showed the ability of nano particulate reinforcements on enhancing strength and/or ductility of magnesium. Commonly, the nanocomposites are synthesized using single ceramic [7–9] or metal reinforcements [10,11]. Reviews of work on particle reinforced magnesium based nanocomposites can be found in recent publications by Dieringa [12] and Ferguson *et al.* [13]. In addition, recent investigations were also made on the magnesium composites containing hybrid particle reinforcements [14–21]. Hybrid reinforcements were prepared by using different combinations such as “ceramic + ceramic”, “ceramic + CNT” and “ceramic + metal” in Mg matrix. Among those combinations, as reported in the previous investigations [12–21], “ceramic + metal” hybrid reinforcements in Mg matrix offered the best improvement in mechanical properties in the related composite systems.

Accordingly, the present study focused on the synthesis of magnesium composites using single ( $ZrO_2$ ) and hybrid ( $ZrO_2 + Cu$ ) reinforcements in nano length scale. The aim is to investigate the effect of addition of nano  $ZrO_2$  and different combination of hybrid reinforcements on the mechanical properties of pure magnesium. Materials synthesis was carried out using the microwave assisted powder metallurgy route. Characterizations on microstructure, hardness, tensile and compressive properties were done on the extruded samples. Particular emphasis was placed to study the effect of single and hybrid reinforcements on the variation in microstructure and mechanical properties of magnesium. Furthermore, the use of different extrusion ratio on the properties of Mg/ $ZrO_2$  composite was also investigated.

## 2. Results and Discussion

### 2.1. Grain Size and Reinforcement Distribution

Grain size measurement results from Table 1 show that there was no significant change in grain size when  $ZrO_2$  reinforcement was present in Mg matrix regardless of the amount of the reinforcement being added. It was realized that, especially for fine particle reinforced composites, grain refinement can only be achieved by using a sufficiently high amount of the reinforcement particles in the matrix material [22]. However, it can be noticed from the current results that matrix grain refinement not only depends on the amount of the reinforcement but also on the particle distribution (Table 1 and Figure 1).

When the ZrO<sub>2</sub> content increased from 0.3 to 1.0 vol % in Mg matrix, the reinforcing particles tend to form larger clusters/agglomerates maintaining the same distribution pattern without dispersing them throughout the matrix (Figure 1a,b). This indicates that the uniformity of particle distribution is insufficient to provide the grain size reduction in all Mg/ZrO<sub>2</sub> compositions. Consequently, the grain size in Mg/ZrO<sub>2</sub> composites remained the same when compared to that of Mg. Also, applying high extrusion ratio (from 20.25:1 to 26:1) has no effect on the grain size variation showing the similar grain size in case of Mg/1.0ZrO<sub>2</sub> composite. But the use of increased extrusion ratio provided better reinforcement distribution as indicated by the smaller space between the clustered nanoparticles shown in Figure 1c. In case of Mg/(ZrO<sub>2</sub> + Cu) hybrid composites, a significant reduction in grain size was observed. The reduction was about one third when compared to that of pure Mg and Mg/ZrO<sub>2</sub> composites. This indicates the usefulness of copper as hybrid reinforcement assisting in the matrix grain refinement. Having limited solid solubility in magnesium, the presence of copper causes Mg<sub>2</sub>Cu intermetallics formation [10,16,23]. The existence of more obstacles (ZrO<sub>2</sub>, Cu and Mg<sub>2</sub>Cu intermetallics) can effectively pin the grain boundary which contributes to the grain size reduction in the hybrid composites. Unlike Mg/ZrO<sub>2</sub> composite, reinforcement distribution was globally finer with increasing presence of second phases in Mg/(ZrO<sub>2</sub> + Cu) composites as observed in the micrograph (Figure 1). The morphology of the Mg/ZrO<sub>2</sub> material shows a more or less continuous film of clustered/agglomerated ZrO<sub>2</sub> nanoparticles at the grain boundaries, whereas in the Cu-containing composite the ZrO<sub>2</sub> film is discontinuous and punctuated with Cu particles. In case of Mg/ZrO<sub>2</sub> composite, the ZrO<sub>2</sub> particles were mostly in the clustered/agglomerated form with minimal particle dispersion within the matrix (Figure 2a).

**Table 1.** Results of grain size and hardness measurements.

Materials (vol %)	Grain size (μm)	Macrohardness (HR15T)	Microhardness (HV)
Mg	25 ± 7	44.7 ± 1.0	42.0 ± 1.6
Mg/0.3ZrO <sub>2</sub>	24 ± 7	46.3 ± 0.9	40.0 ± 1.0
Mg/0.6ZrO <sub>2</sub>	29 ± 3	46.0 ± 2.0	41.6 ± 2.1
Mg/1.0ZrO <sub>2</sub>	25 ± 4	44.1 ± 0.7	42.1 ± 1.9
Mg/1.0ZrO <sub>2</sub> *	23 ± 6	41.8 ± 0.8	39.9 ± 1.4
Mg/(0.3ZrO <sub>2</sub> + 0.7Cu)	9 ± 2	57.9 ± 1.3	47.6 ± 1.0
Mg/(0.6ZrO <sub>2</sub> + 0.4Cu)	11 ± 3	61.1 ± 0.6	50.2 ± 0.9

\* Extrusion ratio of 26:1 was used for this composite.

## 2.2. XRD Analysis

Figure 3 shows the X-ray diffraction patterns of Mg and Mg composites. In case of Mg/1.0ZrO<sub>2</sub> composites, an additional peak of ZrO<sub>2</sub> was revealed when compared to Mg and Mg/(ZrO<sub>2</sub> + Cu) composites. In case of Mg/(ZrO<sub>2</sub> + Cu) composites, the peak related to ZrO<sub>2</sub> was not present. However, the peaks matching to Cu and Mg<sub>2</sub>Cu were found in the XRD patterns. From the related studies [9,24], the peaks related to the ceramic reinforcement particles which are in nano length scale do not generally appear in the composites. This is due to either the amount of reinforcement being too small (less than 2 vol %) to be detected by the XRD diffractometer or the presence of fine

reinforcement particles which are individually or uniformly distributed with small clusters in the matrix [25,26]. It has also been reported in previous studies [25,26] that peaks are normally detectable for the small additions of micron-sized reinforcement particles. It may thus be concluded from the current study that the appearance of  $ZrO_2$  peak in the  $Mg/1.0ZrO_2$  composites is due to the clustered/agglomerated particles as observed in the micrographs (Figure 2a,c). In  $Mg/(ZrO_2 + Cu)$  composites, clustering tendency of  $ZrO_2$  reinforcement was less as discussed in the above section (Section 3.1). The evidence of smaller  $ZrO_2$  clusters and dispersed  $ZrO_2$  particles can also be seen in the micrograph (Figure 2b) which again supports the reason for the absence of  $ZrO_2$  peak in  $Mg/(ZrO_2 + Cu)$  composites. On the other hand, the presence of agglomerated Cu and  $Mg_2Cu$  phase was confirmed by XRD analysis (Figure 3) and EDS analysis (Figure 2d).

**Figure 1.** Field Emission Scanning Electron Microscope (FESEM) micrographs showing second phase distribution in: (a)  $Mg/0.3ZrO_2$ ; (b)  $Mg/1.0ZrO_2$  (20.25:1); (c)  $Mg/1.0ZrO_2$  (26:1); and (d)  $Mg/(0.3ZrO_2 + 0.7Cu)$  composites.

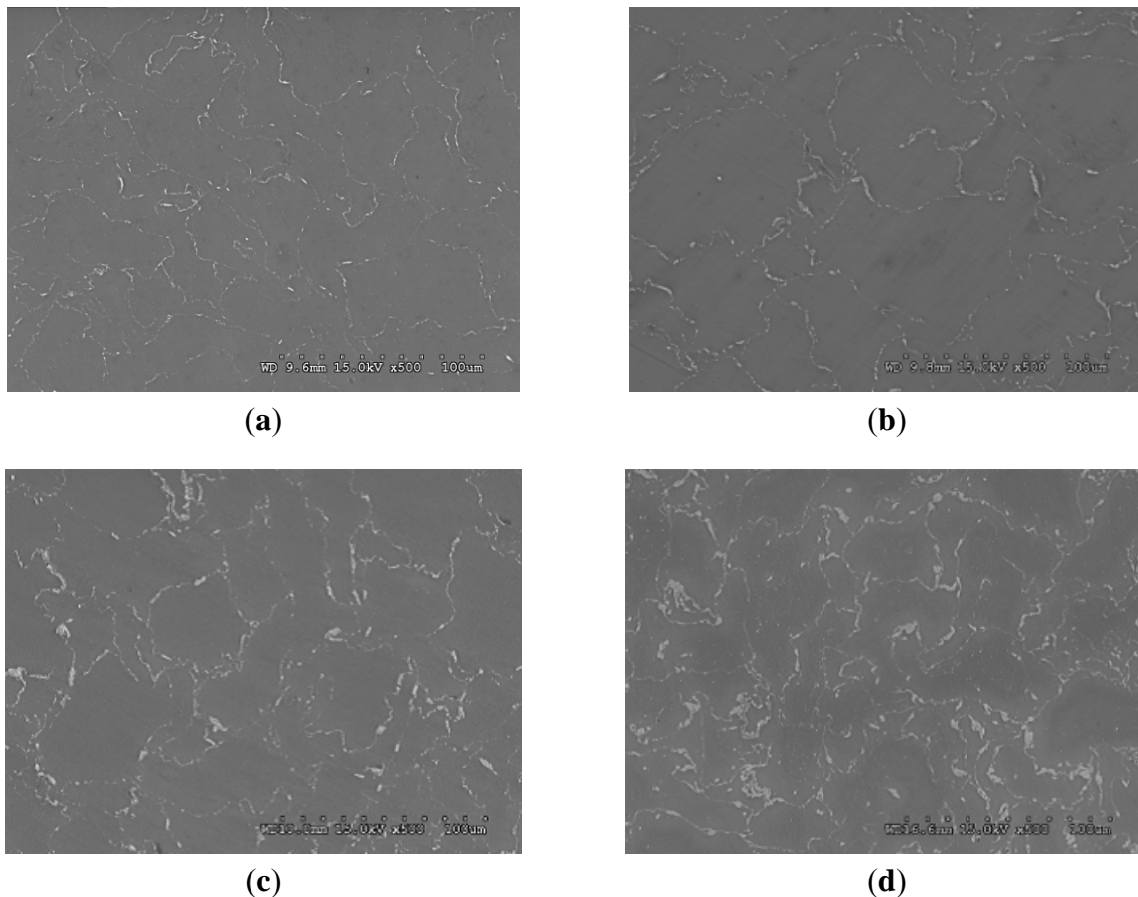


**Figure 2.** Representative micrographs showing: (a) clustered/agglomerated  $ZrO_2$  reinforcements in Mg/1ZrO<sub>2</sub> composite, (b) the presence of Cu, clustered and dispersed  $ZrO_2$  phases in Mg/(0.6ZrO<sub>2</sub> + 0.4Cu) hybrid composite and corresponding energy dispersive X-ray spectroscopy (EDS) analysis in: (c) and (d).

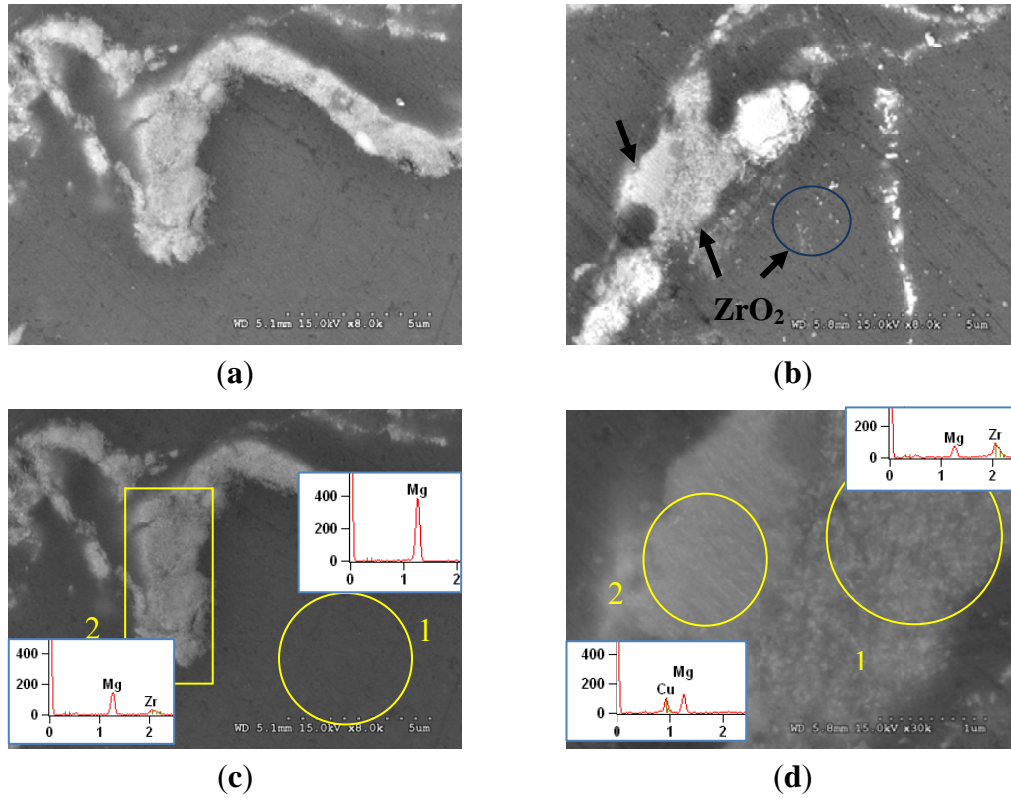
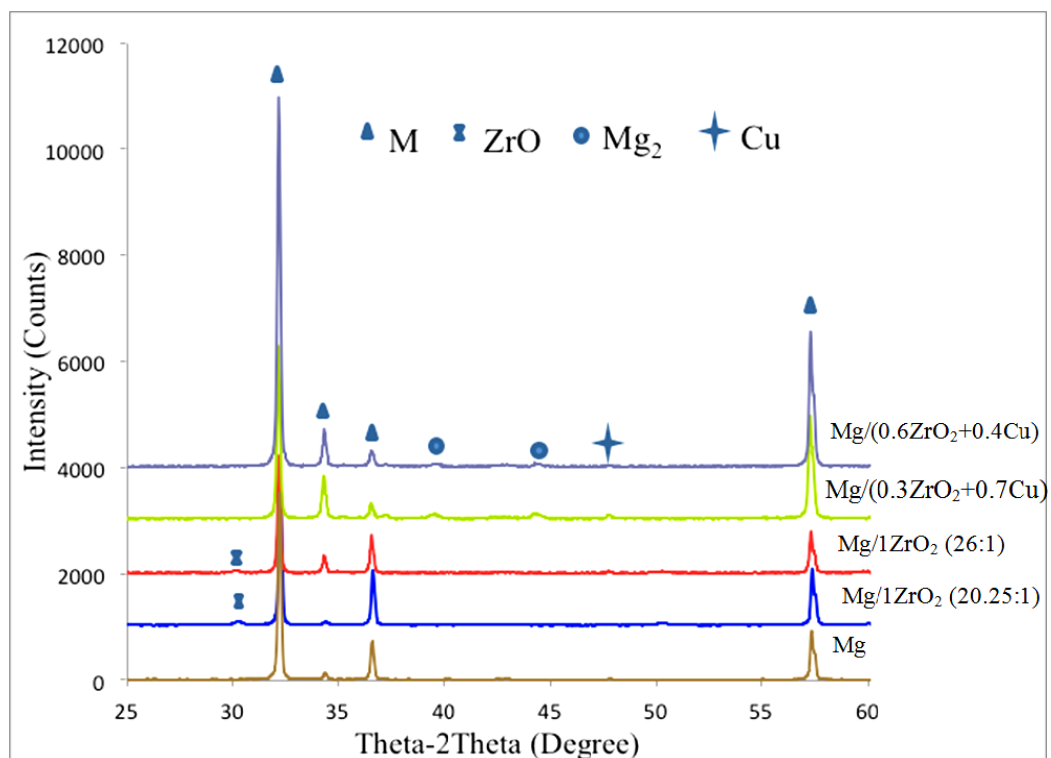


**Figure 3.** X-ray diffractograms of Mg and Mg composites.



### 2.3. Hardness

Hardness measurement results in Table 1 show a minimal change in both macro- and micro- hardness values in the case of pure Mg and Mg/ZrO<sub>2</sub> composites. Results suggest that the presence of single ZrO<sub>2</sub> reinforcement is ineffective in increasing hardness of Mg matrix. This may primarily be attributed to poor reinforcement distribution of ceramic reinforcements. To achieve high hardness level in the composites, clustering of second phases is not preferable due to a number of facts including larger intercluster spacing and the weak bonding among brittle ceramic particulates at the clustered particles region. No variation in hardness can also be attributed to the similar grain size between Mg and Mg/ZrO<sub>2</sub> composites. On the other hand, an improvement in both macro- and micro- hardness was observed in the hybrid composites when compared to both Mg and Mg/ZrO<sub>2</sub> composites. This may primarily be attributed to the grain refinement resulting from the distribution of second phases (Table 1 and Figure 1). The presence of hard Mg<sub>2</sub>Cu intermetallics can additionally provide an increase in hardness level of Mg matrix [27].

### 2.4. Tensile Properties

The results of room temperature tensile properties are shown in Figure 4 and summarized in Table 2. Not only the presence but also the increasing amount of ZrO<sub>2</sub> reinforcement shows no effect on the variation of 0.2% yield and ultimate tensile strengths showing similar strength levels of pure Mg and composite samples. In fact, the strengths in Mg/0.3ZrO<sub>2</sub> and Mg/1.0ZrO<sub>2</sub> composites tend to decrease when compared to pure magnesium. Presence of clustered ZrO<sub>2</sub> particulates in Mg matrix (Figures 1a,b and 2a) could be the prime reason for this decrement. The reduction in strengths originates from weak adhesion among ceramic particulates within clusters and/or between matrix and clustered particulates [4,28]. This also indicates the lack of load transfer from the matrix to ceramic reinforcement clusters and thus yielding in the Mg/ZrO<sub>2</sub> composites follows the matrix yielding behavior that contains defects. The use of high extrusion ratio (20.25:1 to 26:1) provides improvement in both 0.2% yield and ultimate tensile strengths to some extent. This is in line with the improved reinforcement distribution in Mg/1.0ZrO<sub>2</sub> composite with the use of higher extrusion ratio, 26:1 (Figure 1c). However, a significant strength increment was not achieved due to partial break down of reinforcement clusters [29] and lack of grain refinement after applying high extrusion ratio (26:1) in Mg/1.0ZrO<sub>2</sub> composition. Expecting to acquire better tensile properties, Cu was added as hybrid reinforcement to Mg/ZrO<sub>2</sub> compositions. To fix the total reinforcement amount to be 1 vol %, 0.7 vol % and 0.4 vol % Cu were added to the Mg/0.3 vol % ZrO<sub>2</sub> and Mg/0.6 vol % ZrO<sub>2</sub> compositions, respectively. From the tensile test results (Table 2), a significant improvement in both 0.2% yield and ultimate tensile strengths were observed in the hybrid composites. The improvement in strengths can mainly be attributed to: (a) the combined presence of ZrO<sub>2</sub>, Cu and additional Mg<sub>2</sub>Cu intermetallics; (b) effective load transfer from matrix to the reinforcements/second phases conforming uniform reinforcement/second phase distribution; (c) grain refinement as indicated earlier in Table 1. The reduction in grain size is primarily responsible for strength improvement in magnesium hybrid composites. Additionally, the strength increment may be supported by the effective load transfer

mechanism. Irrespective of enhanced tensile strengths shown by the hybrid composites, failure strain is similar to that of pure Mg and Mg/ZrO<sub>2</sub> composites.

**Figure 4.** Representative stress-strain curves of Mg and Mg composites.

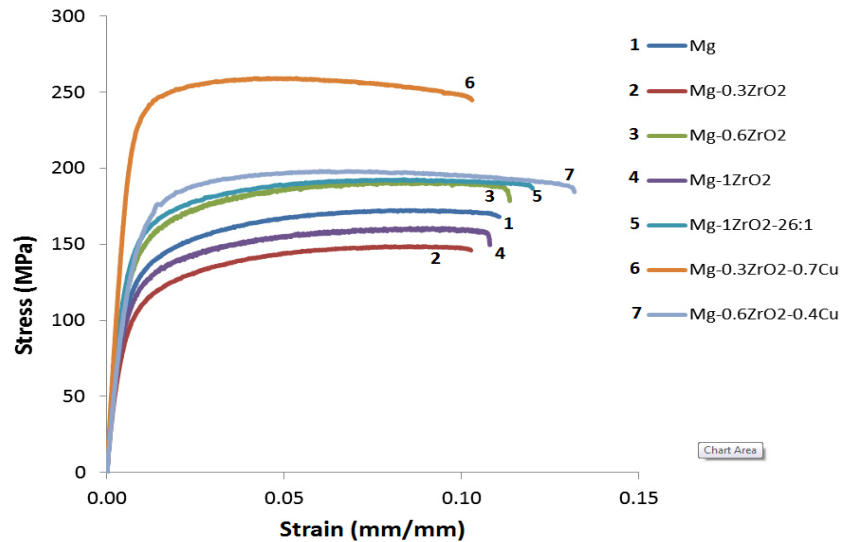


**Table 2.** Results of tensile properties.

Materials (vol %)	0.2% YS (MPa)	UTS (MPa)	Failure Strain (%)
Mg	111 ± 7.8	177 ± 10	9.0 ± 2.2
Mg/0.3ZrO <sub>2</sub>	84.8 ± 8.0	139 ± 7.5	8.1 ± 1.6
Mg/0.6ZrO <sub>2</sub>	117 ± 11	182 ± 14	9.4 ± 2.7
Mg/1.0ZrO <sub>2</sub>	97.8 ± 6.3	158 ± 12	8.6 ± 2.2
Mg/1.0ZrO <sub>2</sub> *	122 ± 7.7	188 ± 5.9	10 ± 1.3
Mg/(0.3ZrO <sub>2</sub> + 0.7Cu)	196 ± 16	249 ± 7.5	8.2 ± 1.1
Mg/(0.6ZrO <sub>2</sub> + 0.4Cu)	139 ± 22	193 ± 21	11.4 ± 2.9

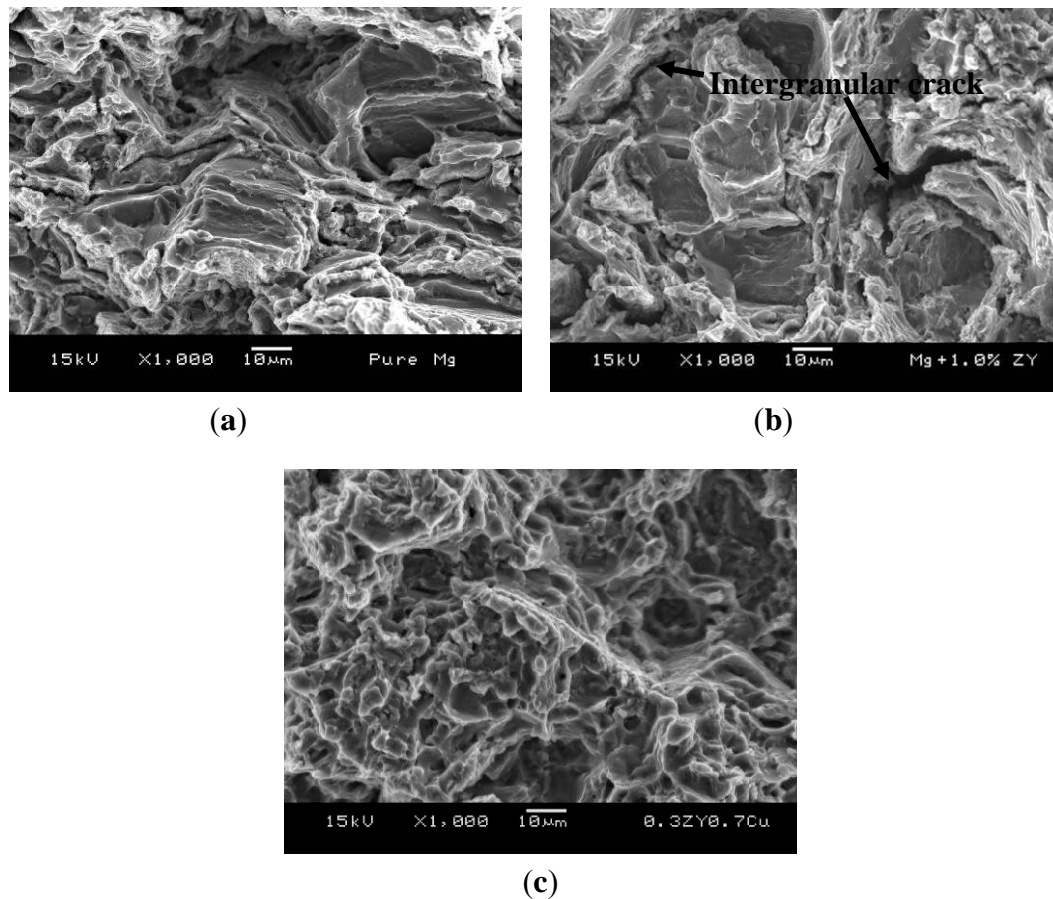
\* Extrusion ratio of 26:1 was used for this composite.

### 2.5. Tensile Fractography

Tensile fractographs can be seen in Figure 5. From the failure analysis, the same fracture features revealing rough fracture surfaces and cleavage fracture were observed in pure Mg and Mg/ZrO<sub>2</sub> composites. Owing to HCP crystal structure, magnesium's deformability is limited due to the lack of sufficient slip activity. Although the size of clustered reinforcements was in micron length scale, premature failure was not observed in the Mg/ZrO<sub>2</sub> composites observing similar failure strain when compared to magnesium (Table 2). This is different from micron size particle reinforced magnesium composites in which failure strain reduction was commonly found when compared to that of unreinforced magnesium. The premature failure in these composites is mainly due to the debonding between the matrix and reinforcement particles, and rapid particle cracking [4]. In the current study, there were two possibilities for Mg/ZrO<sub>2</sub> composite eventual failure: (a) the matrix failure could control the fracture behavior in the composites observing the similar fracture features and (b) failure due to intergranular cracking initiated from micro-cracking of the reinforcement clusters at the grain boundary (Figure 5b). In case of hybrid composite, fine and homogenous fracture features were

observed (Figure 5c). This implies the achievement of high strength in hybrid composites yet the failure strain was not improved (Table 2). This can be primarily attributed to the increasing presence of brittle second phases and the clustered ones remained at the grain boundary.

**Figure 5.** Representative tensile fracture features in: (a) pure Mg; (b) Mg/1.0ZrO<sub>2</sub> (20.25:1) composite; and (c) Mg/(0.3ZrO<sub>2</sub> + 0.7Cu) hybrid composite.



## 2.6. Compressive Properties

Table 3 shows the room temperature compressive properties. From the results, the same compressive yield strength was observed between pure Mg and Mg/ZrO<sub>2</sub> composites while average ultimate compressive strength was marginally reduced in case of Mg/ZrO<sub>2</sub> composites when compared to pure Mg. It is well known that yielding in magnesium materials is mainly due to twinning. Compressive yield strength of magnesium can commonly be increased by reducing the twinning activity through grain refinement [30–32]. In the present study, having similar grain size, compressive yield strength was not improved in Mg/ZrO<sub>2</sub> composites when compared to pure Mg. It also indicates that there was no strengthening effect from the ZrO<sub>2</sub> reinforcement. In case of hybrid composite, both compressive yield and ultimate compressive strengths are significantly increased when compared to Mg and Mg/ZrO<sub>2</sub> composites. This can be mainly attributed to the grain refinement observed in Mg/(ZrO<sub>2</sub> + Cu) composites. For the failure strain in the composites, it was reduced when compared to pure Mg. It suggests that the presence of reinforcement either in the form of single (ZrO<sub>2</sub>) or hybrid (ZrO<sub>2</sub> + Cu) can deteriorate the compressive failure strain of magnesium. From the related

investigations [33,34], it was also found that the compressive failure strain decreased in magnesium composites when compared to its unreinforced counterpart. The resultant failure strain reduction in the current composites is fundamentally in agreement with the observations from the previous studies.

**Table 3.** Results of compressive properties.

Materials * (vol %)	0.2% YS (MPa)	UTS (MPa)	Failure Strain (%)
Mg	109 ± 4	284 ± 11	23 ± 3
Mg/0.3ZrO <sub>2</sub>	109 ± 6	273 ± 13	19 ± 1
Mg/1.0ZrO <sub>2</sub>	109 ± 5	262 ± 18	19 ± 4
Mg/(0.3 ZrO <sub>2</sub> + 0.7Cu)	124 ± 7	352 ± 18	12 ± 3

\* Extrusion ratio of 20.25:1 was used for all materials.

### 2.7. Compressive Fractography

Compressive fractographs are shown in Figure 6. In case of pure magnesium and Mg/ZrO<sub>2</sub> composites (Figure 6a–c), the fracture surfaces are relatively smooth and the shear band formation can hardly be seen in the failed samples. According to the investigation from Ion *et al.* [35] on single phase Mg alloy, shear band formation was due to heterogeneous deformation in materials arising from localized deformation at grain boundary leaving cores of the grains undeformed under compressive loading. The minimal presence of shear bands in pure Mg indicates that there was homogenous deformation due to the presence of fewer obstacles through less grain boundary area and absence of secondary phases. This deformation mechanism can also be applied to the Mg/ZrO<sub>2</sub> composites having similar grain size and minimal or the lack of dispersion of ZrO<sub>2</sub> particles within the grain interior (Figure 2a,c). In contrast, heterogeneous fracture surface and the presence of shear bands are found in Mg/(ZrO<sub>2</sub>+Cu) hybrid composite (Figure 6d). The plastic deformation in the hybrid composite was constrained due to the presence of dispersed second phases and comparatively large amount of grain boundaries. This led to the significant reduction in compressive failure strain in the hybrid composite (Table 3).

**Figure 6.** Representative compressive fractographs of: (a) pure Mg; (b) Mg/0.3ZrO<sub>2</sub>; (c) Mg/1.0ZrO<sub>2</sub> and (d) Mg/(0.3ZrO<sub>2</sub> + 0.7Cu) composites.

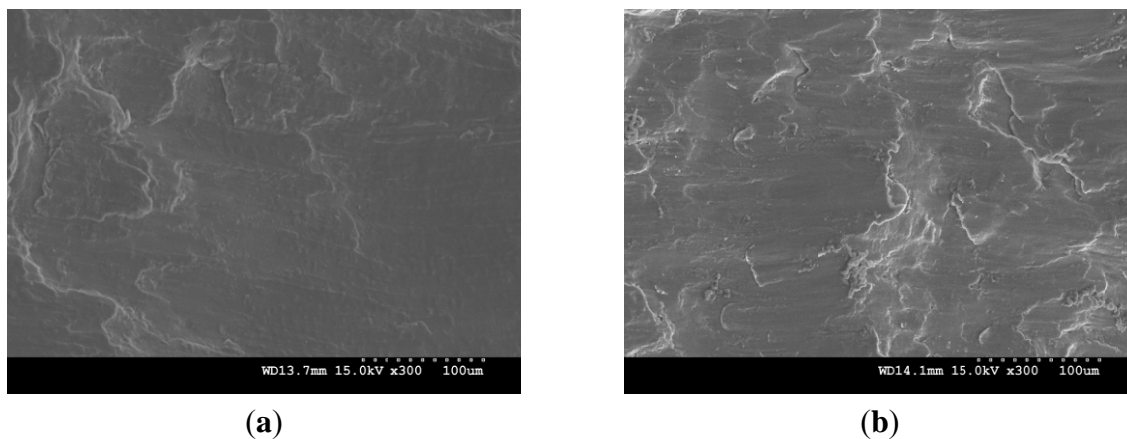
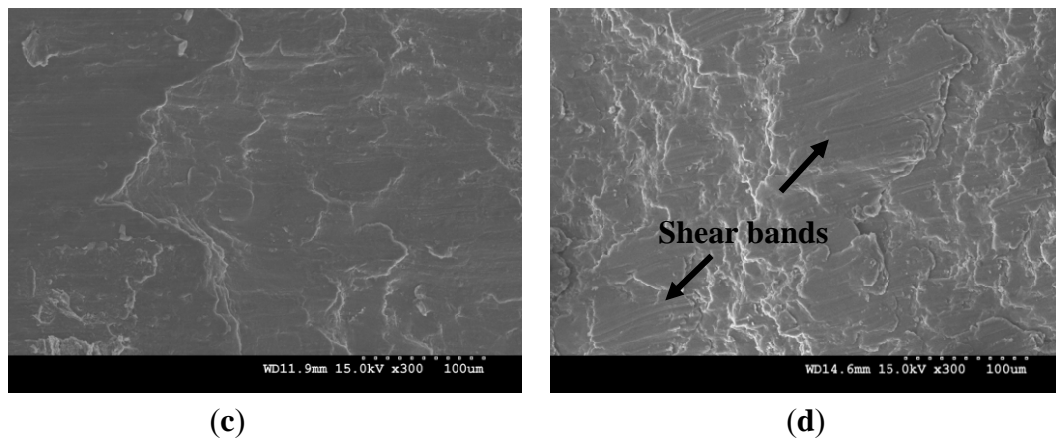


Figure 6. Cont.



### 3. Experimental Section

#### 3.1. Materials

The material used for the matrix is magnesium (Mg) powder of 98.5% purity with particle sizes ranging from 60 to 300  $\mu\text{m}$  (Merck, Germany). As for the reinforcements, yttria-stabilized Zirconia ( $\text{ZrO}_2$ ) of 99.9% purity with particle sizes ranging from 51 to 65 nm and copper (Cu) of 99.8% purity with an average particle size of 25 nm (Nanostructured & Amorphous Materials, Inc., TX, USA) were used.

#### 3.2. Processing

The primary processing for the composites was done in sequential order of blending, pressing and sintering according to the powder metallurgy technique. Magnesium and reinforcement powders were first weighed in accordance with the designated compositions; Mg/0.3 vol %  $\text{ZrO}_2$ , Mg/0.6 vol %  $\text{ZrO}_2$ , Mg/1.0 vol %  $\text{ZrO}_2$ , Mg/(0.3 vol %  $\text{ZrO}_2$  + 0.7 vol % Cu) and Mg/(0.6 vol %  $\text{ZrO}_2$  + 0.4 vol % Cu). The powder mixture was then blended using planetary ball milling machine at 200 rpm for 1 h followed by cold compaction. No balls or process control agent was used during the blending step. Compaction was done at a pressure of 97 bars (510 MPa) to form billets of 35 mm diameter and 40 mm height using a 100 ton press. Monolithic magnesium was compacted using the same parameters but without blending. The compacted billets were sintered using a hybrid microwave sintering technique to a temperature near the melting point of magnesium ( $\sim 640$  °C) in a 900 W, 2.45 GHz SHARP microwave oven. Microwave sintering was carried out in ambient atmospheric conditions.

The secondary processing involved the hot extrusion of the sintered billets. The sintered billets were subsequently hot extruded at a temperature of 350 °C at an extrusion ratio of 20.25:1 to produce 8 mm diameter extruded rods. During extrusion of Mg/1.0 vol %  $\text{ZrO}_2$  composition, two different extrusion ratios, 20.25:1 and 26:1 were used. Prior to extrusion, the sintered billets were soaked in a resistance furnace at a temperature of 400 °C for 1 h.

### 3.3. Microstructure Characterization

Microstructural characterization studies were conducted to determine the grain size and distribution of reinforcements. OLYMPUS metallographic optical microscope, Scion Image Analyzer and HITACHI S-4300 Field Emission Scanning Electron Microscope (FESEM) equipped with energy dispersive X-ray spectroscopy (EDS) were used for this purpose.

### 3.4. X-ray Diffraction Studies

X-ray diffraction analysis was carried out on the polished extruded Mg and Mg composite samples using automated Shimadzu LAB-X XRD-6000 diffractometer. The samples were exposed to  $\text{CuK}\alpha$  radiation ( $\lambda = 1.54056 \text{ \AA}$ ) at a scanning speed of  $2 \text{ }^\circ\text{C}/\text{min}$ . The Bragg angle and the values of the interplanar spacing ( $d$ ) obtained were subsequently matched with the standard values for Mg,  $\text{ZrO}_2$ , Cu and related phases.

### 3.5. Mechanical Testing

The mechanical behavior of both monolithic and composite samples was quantified in terms of hardness, tensile and compressive properties. Macrohardness measurements were made using Future-Tech FR-3 Rockwell Type Hardness Tester. The test was conducted under conditions of 2 s dwell time and a test load of 15 kgf using steel ball indenter (1.588 mm) in accordance with ASTM E18-02. Microhardness measurements were performed on the magnesium matrix of the polished samples using Shimadzu-HMV automatic digital microhardness tester. The test was done using a Vickers indenter under a test load of 25 gf and a dwell time of 15 s in accordance with the ASTM standard E384-99.

The tensile properties of the as-extruded monolithic magnesium and its composite counterparts were determined in accordance with procedures outlined in ASTM standard E8M-01. The tensile tests were conducted on round tension test specimens (5-mm gage diameter and 25-mm gage length) on MTS 810 automated servo-hydraulic mechanical testing machine at a crosshead speed set at 0.254 mm/min.

Compression tests were performed on cylindrical monolithic and composite samples according to ASTM E9-89a using MTS 810 automated servo-hydraulic mechanical testing. Extruded rod of 8 mm diameter was cut into 8 mm length samples for compression tests to provide the aspect ratio ( $l/d$ ) of unity. Samples were tested at a strain rate of  $5 \times 10^{-3} \text{ min}^{-1}$  and the compression load was applied parallel to the extrusion direction.

### 3.6. Fracture Behavior

To investigate the failure mechanism during tensile and compressive loadings, the tensile and compressive fractured surfaces of pure Mg and its composite specimens were characterized using scanning electron microscope (SEM).

#### 4. Conclusions

The major conclusions are as follows:

1. Magnesium based nanocomposites and hybrid composites can be successfully synthesized using microwave sintering assisted powder metallurgy approach.
2. The formation of ZrO<sub>2</sub> reinforcement clusters in Mg matrix resulted in the lack of grain refinement in all Mg/ZrO<sub>2</sub> composite compositions. On the other hand, the use of hybrid reinforcements (ZrO<sub>2</sub> + Cu) realized significant grain size reduction in magnesium hybrid composites.
3. Both macro- and micro-hardness, tensile, and compressive strengths were improved only in the Mg/(ZrO<sub>2</sub> + Cu) hybrid composites primarily as a result of their finer grain size.
4. Tensile failure strain remained the same whereas compressive failure strain was decreased in all composites when compared to pure Mg.
5. Tensile failure analysis revealed the similar rough fracture features in the case of Mg and Mg/ZrO<sub>2</sub> composites. Refined fracture features were observed in the hybrid composite.
6. Under compressive loading, the presence of shear bands was minimally observed from the fracture surfaces of Mg and Mg/ZrO<sub>2</sub> composites. In case of hybrid composite, a large amount of shear band formation was observed.

#### Acknowledgments

Authors wish to acknowledge Qatar National Research Fund (QNRF), Qatar (NPRP 08-424-2-171) for supporting this research.

#### References

1. Kainer, K.U.; Buch, F. The Current State of Technology and Potential for further Development of Magnesium Applications. In *Magnesium Alloys and Technology*; Wiley-VCH: Weinheim, Germany, 2003; pp. 1–22.
2. Housh, S.; Mikucki, B.; Stevenson, A. Selection and Application of Magnesium and Magnesium Alloys. In *ASM Handbook*, 10th ed.; ASM International: Materials Park, OH, USA, 1990; Volume 2, pp. 455–479.
3. Moll, F.; Kainer, K.U. Particle-Reinforced Magnesium Alloys. In *Magnesium Alloys and Technology*; Wiley-VCH: Weinheim, Germany, 2003; pp. 197–217.
4. Lloyd, D.J. Particle reinforced aluminium and magnesium matrix composites. *Int. Mater. Rev.* **1994**, *39*, 1–23.
5. Ye, H.Z.; Liu, X.Y. Review of recent studies in magnesium matrix composites. *J. Mater. Sci.* **2004**, *39*, 6153–6171.
6. Tjong, S.C. Novel nanoparticle reinforced metal matrix composites with enhanced mechanical properties. *Adv. Eng. Mater.* **2007**, *9*, 639–652.
7. Hassan, S.F.; Gupta, M. Development of high performance Mg nanocomposites using nano-Al<sub>2</sub>O<sub>3</sub> as reinforcement. *Mater. Sci. Eng. A* **2005**, *392*, 163–168.
8. Goh, C.S.; Wei, J.; Lee, L.C.; Gupta, M. Properties and deformation behaviour of Mg–Y<sub>2</sub>O<sub>3</sub> nanocomposites. *Acta Mater.* **2007**, *55*, 5115–5121.

9. Tun, K.S.; Gupta, M. Improving mechanical properties of magnesium using nano-Yttria reinforcement and microwave assisted powder metallurgy method. *Compos. Sci. Technol.* **2007**, *67*, 2657–2664.
10. Wong, W.L.E.; Gupta, M. Development of Mg/Cu nanocomposites using microwave assisted rapid sintering. *Compos. Sci. Technol.* **2007**, *67*, 1541–1552.
11. Zhong, X.L.; Wong, W.L.E.; Gupta, M. Enhancing strength and ductility of magnesium by integrating it with aluminum nanoparticles. *Acta Mater.* **2007**, *55*, 6338–6344.
12. Dieringa, H. Properties of magnesium alloys reinforced with nanoparticles and carbon nanotubes: A review. *J. Mater. Sci.* **2011**, *46*, 289–306.
13. Ferguson, J.B.; Sheykh-Jaberi, F.; Kim, C.S.; Rohatgi, P.K.; Cho, K. On the strength and strain to failure in particle-reinforced magnesium metal-matrix nanocomposites (Mg MMNCs). *Mater. Sci. Eng. A* **2012**, *558*, 193–204.
14. Nguyen, Q.B.; Tun, K.S.; Chan, J.; Kwok, R.; Kuma, J.V.M.; Gupta, M. Enhancing strength and hardness of AZ31B through simultaneous addition of nickel and nano- $\text{Al}_2\text{O}_3$  particulates. *Mater. Sci. Eng. A* **2011**, *528*, 888–894.
15. Nguyen, Q.B.; Tun, K.S.; Chan, J.; Kwok, R.; Kumar, J.V.M.; Phung, H.T.; Gupta, M. Simultaneous effect of nano- $\text{Al}_2\text{O}_3$  and micron-Cu Particulates on microstructure and mechanical properties of magnesium alloy AZ31. *Mater. Sci. Technol.* **2012**, *28*, 227–233.
16. Tun, K.S.; Gupta, M.; Srivatsan, T.S. Investigating influence of hybrid (yttria + copper) nanoparticulate reinforcements on microstructural development and tensile response of magnesium. *Mater. Sci. Technol.* **2010**, *26*, 87–94.
17. Tun, K.S.; Gupta, M. Development of magnesium (Yttria + Nickel) hybrid nanocomposites using hybrid microwave sintering: Microstructure and tensile properties. *J. Alloys Compd.* **2009**, *487*, 76–82.
18. Thakur, S.K.; Balasubramanian, K.; Gupta, M. Microwave synthesis and characterization of magnesium based composites containing nanosized SiC and hybrid ( $\text{SiC} + \text{Al}_2\text{O}_3$ ) reinforcements. *Trans. ASME* **2007**, *129*, 194–199.
19. Thakur, S.K.; Srivatsan, T.S.; Gupta, M. Synthesis and mechanical behavior of carbon nanotube-magnesium composites hybridized with nanoparticles of alumina. *Mater. Sci. Eng. A* **2007**, *466*, 32–37.
20. Wong, W.L.E.; Karthik, S.; Gupta, M. Development of hybrid Mg/ $\text{Al}_2\text{O}_3$  composites with improved properties using microwave assisted rapid sintering route. *J. Mater. Sci.* **2005**, *40*, 3395–3402.
21. Wong, W.L.E.; Gupta, M. Effect of hybrid length scales (micro + nano) of SiC reinforcement on the properties of magnesium. *Solid State Phenom.* **2006**, *111*, 91–94.
22. Kang, Y.C.; Chan, S.L. Tensile properties of nanometric  $\text{Al}_2\text{O}_3$  particulate-reinforced aluminum matrix composites. *Mater. Chem. Phys.* **2004**, *85*, 438–443.
23. Okamoto, H. *ASM Desk Handbook: Phase Diagram for Binary Alloys*; ASM International: Materials Park, OH, USA, 2000; p. 301.
24. Wong, W.L.E.; Gupta, M. Improving overall mechanical performance of magnesium using nano-alumina reinforcement and energy efficient microwave assisted processing route. *Adv. Eng. Mater.* **2007**, *9*, 902–909.
25. Suryanarayana, C. Mechanical alloying and milling. *Prog. Mater. Sci.* **2001**, *46*, 1–25.

26. Cullity, B.D. *Element of X-ray Diffraction*, 2nd ed.; Addison-Wesley: Reading, MA, USA, 1978; p. 414.
27. Westbrook, J.H. *Intermetallic Compounds*; John Wiley & Sons: New York, NY, USA, 1967; p. 471.
28. Tham, L.M.; Gupta, M.; Cheng, L. Effect of limited matrix-reinforcement interfacial reaction on enhancing the mechanical properties of aluminium-silicon carbide composites. *Acta Mater.* **2001**, *49*, 3243–3253.
29. McDanel, D.L. Analysis of stress-strain fracture and ductility behavior of Al-matrix composites containing discontinuously SiC reinforcement. *Metall. Trans. A* **1985**, *16A*, 1105–1115.
30. Barnett, M.R.; Keshavarz, Z.; Beer, A.G.; Atwell, D. Influence of grain size on the compressive deformation of wrought Mg–3Al–1Zn. *Acta Mater.* **2004**, *52*, 5093–5103.
31. Meyers, M.A.; Vohringer, O.; Lubarda, V.A. The onset of twinning in metals: A Constitutive Description. *Acta Mater.* **2001**, *49*, 4025–4039.
32. Yang, H.; Yin, S.; Huang, C.; Zhang, Z.; Wu, S.; Li, S.; Liu, Y. EBSD study on deformation twinning in AZ31 magnesium alloy during quasi-*in-situ* compression. *Adv. Eng. Mater.* **2008**, *10*, 955–960.
33. Towle, D.J.; Friend, C.M. Comparison of compressive and tensile properties of magnesium based metal matrix composites. *Mater. Sci. Technol.* **1993**, *9*, 35–41.
34. Li, J.Q.; Wang, L.; Cheng, H.W.; Zhang, H.F.; Hu, Z.Q.; Cai, H.N. Synthesis and compressive deformation of rapidly solidified magnesium alloy and composites reinforced by SiC<sub>p</sub>. *Mater. Sci. Eng. A* **2008**, *474*, 24–29.
35. Ion, S.E.; Humphreys, F.J.; White, S.H. Dynamic recrystallisation and the development of microstructure during the high temperature deformation of magnesium. *Acta Metall.* **1982**, *30*, 1909–1919.

© 2013 by the authors; licensee MDPI, Basel, Switzerland. This article is an open access article distributed under the terms and conditions of the Creative Commons Attribution license (<http://creativecommons.org/licenses/by/3.0/>).